Monitoring of sugars adsorption breakthrough curves with online Raman spectroscopy

Wassim Ammar, Marion Lacoue-Negre, Alain Methivier, Maria Manko

Spectrochimica Acta Part A: Molecular and Biomolecular Spectroscopy 309 (2024) 123868

Contents lists available at ScienceDirect

Spectrochimica Acta Part A:
Molecular and Biomolecular Spectroscopy

journal homepage: www.journals.elsevier.com/spectrochimica-acta-part-a-molecular-and-biomolecular-spectroscopy

Monitoring of sugars adsorption breakthrough curves with online Raman spectroscopy

Wassim Ammar, Marion Lacoue-Negre, Alain Methivier, Maria Manko *

IFP Energies nouvelles, Rond-point de l'échangeur de Solaize, 69360 Solaize, France

HIGHLIGHTS

- Raman spectroscopy for online monitoring of sugars separation.
- Accurate breakthrough curves predictions with univariate and PLS models.
- Spectra pretreatment essential to enhance accuracy and avoid overlaps.

GRAPHICAL ABSTRACT

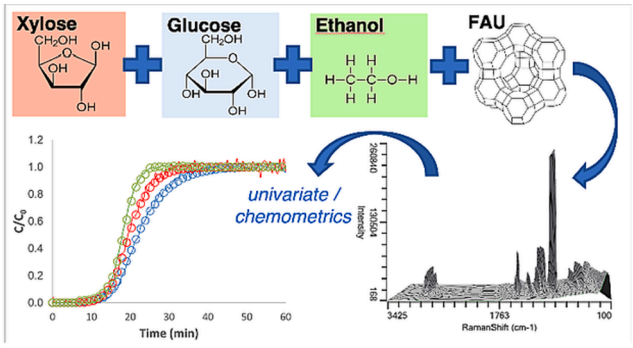

ARTICLE INFO

Keywords:
Raman Spectroscopy
Adsorption
Breakthrough Curve
Online Monitoring
Sugars
PLS model

ABSTRACT

We introduce a new application for online Raman spectroscopy to monitor adsorption breakthrough curves of a glucose and xylose mixtures. Univariate and multivariate Partial Least Squares (PLS) calibration models are developed for each sugar when they are dissolved in water and in the case of the ethanol addition as a cosolvent. The models are validated by performing actual breakthrough experiments in a liquid phase using a column packed with a zeolite adsorbent. The first statistical moments of predicted curves are compared to the reference curves obtained with offline High-Performance Liquid Chromatography (HPLC). Glucose and xylose univariate predictions in the presence or absence of ethanol in the mixture are accurate and no improvements are found with the PLS models. Spectral subtraction coupled with the first derivative proved to be effective pretreatments to develop robust univariate models.

1. Introduction

Lignocellulosic biomass is considered as valuable renewable feedstock to produce fuels and chemicals [1,2]. It is composed of three main constituents, (i) cellulose a polymer of glucose molecules, hexoses ($C_6H_{12}O_6$), (ii) hemicellulose a polymer chain of several pentoses ($C_5H_{10}O_5$), and hexoses such as mannose, arabinose, and xylose, (iii) lignin a polyphenolic compound [3]. The chemical composition differs from one vegetal specie to another but overall, glucose and xylose are the major monosaccharides present in lignocellulosic biomass [3].

* Corresponding author at: IFP Energies nouvelles, Rond-point de l'échangeur de Solaize, 69360 Solaize, France.
E-mail address: maria.manko@ifpen.fr (M. Manko).

https://doi.org/10.1016/j.saa.2024.123868
Received 21 June 2023; Received in revised form 4 January 2024; Accepted 5 January 2024
Available online 11 January 2024

Today, the mixture of sugars is commonly transformed by fermentation into alcohol. However, the other and more valuable way of their application is to extract pure single monosaccharides to convert them into high value-added chemicals. Reactions starting from a pure sugar yield better conversion rates and higher selectivities towards the desired products, such as ethylene glycol from glucose transformation or furfural obtained from xylose [4,5]. A separation step of the sugars mixture is therefore necessary. The most cited separation methods which found applications for sugars are filtration and adsorption. Nanofiltration on piperazine-based membranes is reported to be an efficient method to separate glucose and xylose from concentrated monosaccharide solutions [6,7]. However, chromatographic adsorption with a Simulated Moving Bed process (SMB) is employed at an industrial scale to separate glucose and fructose to produce high fructose corn syrup (HFCS) for the food industry [9,8]. Compared to nanofiltration, the SMB process is more efficient and can achieve 99.9 % of purity while the first does not exceed 99.4 % [10].

Separation based on adsorption is investigated in literature for many monosaccharides and disaccharides [11–13]. using different adsorbents (resins, zeolites, active carbons, and amorphous silicas). Two methods are mainly used to perform adsorption experiments. The first is called the “batch test”, which is a simple way to study the adsorption capacity of different adsorbents by mixing a solid with a feed solution (ex. sugar in water) over a fixed period time and constant temperature. The concentration variation is measured before and after adsorption occurred [15,14] The second way, which is closer to industrial continuous conditions, is known as the “breakthrough experiment”. It consists in pumping the feed solution through a fixed bed (column packed with an adsorbent) and recording the concentration profile at the column outlet. Plotting the concentration as a function of time results in a breakthrough curve, from which valuable information about the adsorption process can be explored like thermodynamic parameters (adsorption heat, selectivity and capacity) and mass transfer coefficients [16]. Determination of the first statistical moment (μ) in particular allows to calculate the adsorption capacity, i.e. the adsorbed amount of sugar per mass of adsorbent [17]. In general, offline analytical methods are often used to measure the concentration of the adsorbed species by analyzing the samples collected at the column’s outlet. High Performance Liquid Chromatography (HPLC) is considered as the reference technique for frontal adsorption tests in the liquid phase thanks to its robustness and reliable results. Nevertheless, this conventional approach is costly in consumables and time analysis, requiring sampling device and samples preparation before analyzing them (filtration, dilution, internal standard, or even a reagent addition). Online techniques are often an alternative for this kind of application, they provide immediate responses and data ready to be analyzed. For a single component sugar aqueous solution, online refractive index (RI) detectors were used to study the adsorption of sugars (glucose or fructose) for breakthrough experiments [16,19,18]. However, this method is limited to monitor sugar mixtures since glucose and fructose have the same refractive indexes regardless of the concentration. Offline HPLC is then used to obtain the sugar concentration [20].

Online spectroscopy is advantageous compared to offline analysis in breakthrough tests application. It provides quick reliable data ready to be treated and especially it is cost effective due to the reduction of consumables usage. Optical spectroscopy in particular is a powerful tool for the online monitoring, identification, and quantification of chemicals in complex systems [21]. Fourier transform Mid-infrared spectroscopy (MIR) and Near-infrared (NIR) spectroscopy for instance have found large applications in bioprocess, medical or pharmaceutical fields. They are nondestructive, do not require sample preparation, rapid, robust, and easily implemented for online analysis thanks to the use of optical fiber [22].

Regarding vibrational spectroscopies, Raman spectroscopy showed promising results in analyzing lignocellulosic components. In addition to having the same advantages as infrared spectroscopies, the analyte spectra are not hindered by the presence of water. Biomass treatment has been successfully followed with different Raman techniques in real time to monitor cellulose and lignin, especially in the objective of proposing better pretreatments to maximize yields [23,24]. Shih et al. reported good quantification of glucose and xylose in hydrolysates obtained with acidic and basic treatments using univariate and PLS regression methods [25]. The most common application employing online Raman spectroscopy is the fermentation of sugars into ethanol, simple systems with a single carbon source, usually glucose, showed good agreement with offline monitoring [27,26,28]. Gray et al. studied corn mash fermentation under industrial conditions. Starch, dextrins, maltotriose, maltose, glucose, and ethanol were monitored using chemometric modeling and the authors reported accurate predictions for this complex system [29].

In this work, Raman spectroscopy is used for the first time to our knowledge to monitor breakthrough curves of sugars’ aqueous mixtures, mainly glucose, and xylose, with or without ethanol as cosolvent. The aim of this investigation is to compare the efficiency of models developed by multivariate calibration, based on the PLS algorithm, with univariate linear regression models for the quantification of sugars during breakthrough experiments. Predictions of breakthrough curves are then compared to HPLC ones.

2. Methods

2.1. Breakthrough experiments

Zeolite NaY provided by Arkema was exchanged into barium form (BaY) and packed into a 25 cm length column with an internal diameter of 0.77 cm. The column was then placed inside an oven in the breakthrough tests unit presented in Fig. 1. The setup was composed of two pumps, (SHIMADZU LC-40D) the first to deliver the feed solution and the second to pump the eluent for the regeneration step (ultrapure water in this case). Feed solutions were aqueous mixtures of glucose or xylose dissolved in water with or without ethanol as cosolvent. D-glucose and D-xylose were purchased from Sigma-Aldrich with a purity > 99 % and absolute ethanol from VWR. At the column outlet, a Raman probe was placed, and a fractions collector (GILSON 206 fraction collector) was installed at the end of the line to collect samples and determine the concentrations also with HPLC.

The adsorbent was initially hydrated by filling the column with water at room temperature. Then the feed solution was injected. When the adsorption equilibrium was established, (i.e. when the breakthrough curve reaches a plateau and the recorded concentration is the same as the feed) a four way valve was turned and water was pumped to desorb the sugar molecules from the solid. Plotting the column outlet concentration as a function of time gives a breakthrough curve from which the retention time, also known as the first statistical moment, is determined. The first moment μ (min) was calculated thanks the trapezoidal iterative integration method with the following equation:

$$\mu = \int_0^{\infty} \left(1 - \frac{C(t)}{C_0}\right) dt \tag{1}$$

where $C(t)$ is the concentration of a given species at the column outlet at time t, C_0 is the concentration of a given species in the feed.

2.2. Raman spectroscopy

The Raman measurements were carried out using a dispersive spectrometer RXN2 from Endress + Hauser equipped with a 785 nm diode laser and a Peltier cooled charge coupled device (CCD) array detector. The optic fiber was connected to a Process Elite Flowcell Ballprobe® from Marqmetrix placed at the column’s outlet. Data acquisition was performed using IC Raman 4.4, spectra were collected in a spectral range from 100 to 3400 cm^{-1}. The exposure time was 14 s, and 2

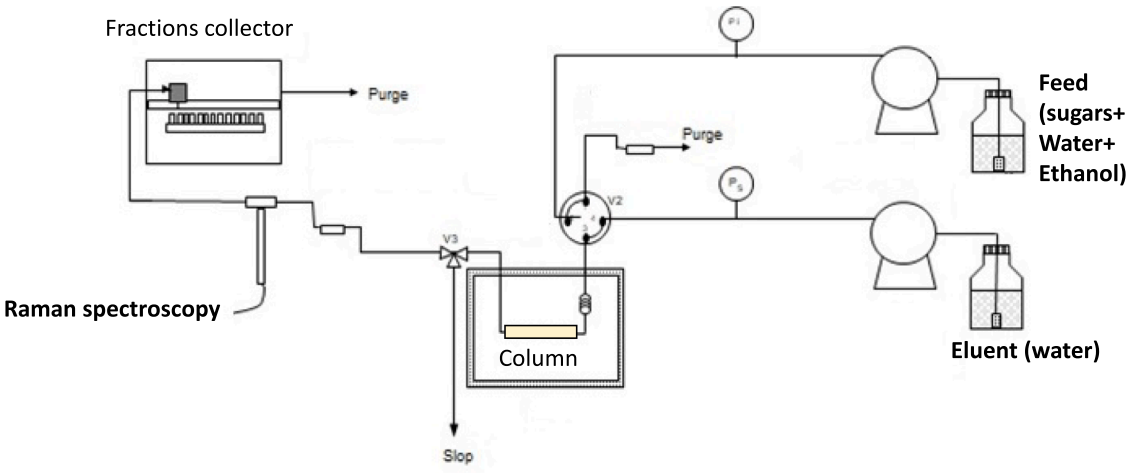

Fig. 1. Adsorption breakthrough tests unit.

accumulations were performed for each spectrum. Cosmic ray filter was applied as well.

2.3. HPLC

Samples were injected (20 µl) into a REZEX RCM-Monosaccharide Ca^{2+} (8 %) column. The mobile phase (ultrapure water, obtained with a Millipore Milli-Q® lab water system) was pumped thanks to Waters 1515 isocratic pump with a flow rate of 0.6 mL.min^{-1}. Waters 2414 refractive index detector was used, and the temperature of the column was 90 °C.

2.4. Modeling

In this work two approaches of modeling were tested: a univariate and a multivariate one with two different systems. The first system was composed of glucose and xylose dissolved in water and the second was additionally enriched with a co-solvent, ethanol. The spectral regions used for pretreatment were specific depending on the system.

2.4.1. Databases

Two systems were of interest in the study. The first was the adsorption from a mixture of glucose and xylose in BaY when the sugars were only dissolved in water. 36 aqueous standard sugars solutions with concentrations from 15 g·kg^{-1} to 250 g·kg^{-1} were used to build the calibration model.

The second system was the same two sugars adsorption in presence of ethanol as a cosolvent. 32 standard solutions were considered with sugars concentrations ranging from 5 g·kg^{-1} to 150 g·kg^{-1}. Ethanol content was between 1 % and 60 % corresponding to concentrations in the range of 10 g·kg^{-1} and 480 g·kg^{-1}.

Single component solutions and mixtures (binary and ternary in presence of ethanol) were used in both systems for the calibration sets. All reference concentrations for the two systems were measured with a Mettler Toledo semi-microbalance MS with a precision of 0.1 mg.

Two breakthrough experiments were performed for validation. The first test was done with an aqueous mixture of 100 g·kg^{-1} glucose and 100 g·kg^{-1} xylose, and the second with 100 g·kg^{-1} glucose, 100 g·kg^{-1} xylose and 50 g·kg^{-1} of ethanol. The predicted concentrations coming from the application of univariate and multivariate models on the spectra recorded during these tests were compared with HPLC measurements. The first moments µ (min) calculated with each model were confronted to the HPLC ones considered as validation references.

2.4.2. Univariate modeling

Univariate modeling for glucose and xylose in the first system was done by taking the height of the peaks between 974 and 1000 cm^{-1} for xylose and between 1128 and 1217 cm^{-1} for glucose. Peaks in the spectral regions 603–635 cm^{-1}, 878–895 cm^{-1} and 1124–1192 cm^{-1} were considered for xylose, ethanol, and glucose respectively in the second system. Baselines in the same spectral regions were taken to determine the heights. For each model, the spectrum of the 100 g·kg^{-1} solution of the non-targeted sugar was subtracted from all the calibration system as a first step of spectral pretreatment. The first derivative was applied next. These pretreatments resolved peaks overlaps since the two sugars have close chemical structures. Overall, five individual univariate models were developed for the two systems using IC Raman 4.4. The Root Mean Square Errors of Calibration (RMSEC) were calculated for all univariate models according to Equation (2) as well as calibration correlation coefficients (R^2).

$$RMSEC = \sqrt{\frac{\sum_{i=1}^{N}(Y_i - \widehat{Y_i})^2}{N}} \quad (2)$$

where Y_i is the reference concentration, $\widehat{Y_i}$ the predicted concentration and N the number of data in the calibration set.

2.4.3. Multivariate modeling

Raman spectra were exported from IC Raman to PLS_Toolbox version 9.0 (Eigenvector) for MATLAB (R2021b version) to develop the multivariate models. The PLS regression was used [30]. The spectral region 250–1600 cm^{-1} was used to model glucose and xylose in both systems, whereas the information between 800 and 1600 cm^{-1} was considered for ethanol. The pretreatment of the spectra was adapted for the PLS modeling, and different from the univariate modeling. No spectral subtraction was done on the spectra prior to PLS modeling. For all models, a Savitzky-Golay first derivative (window points: 15 and order: 2) was used as pretreatment on the raw spectra. The optimal number of latent variables (LV) was selected considering the values of Root Mean Square Error of Cross Validation (RMSECV) obtained by cross validation of calibration data. Venetian blinds cross-validation was applied using 2 splits for glucose and xylose in the first system and 2, 10 and 4 splits for glucose, xylose, and ethanol respectively for the second. The RMSEC and R^2 were also calculated for each multivariate model.

3. Results and discussion

3.1. Spectral interpretation

Developing reliable models requires as a first step an analysis of spectral data. The spectra acquired for the first system composed of glucose and xylose dissolved in water are displayed in SM (**Figure S.1**) in the spectral region 100–1600 cm^{-1} showing the quality of the signal and the complexity of the spectra with overlapped bands. To pinpoint the bands related to each component of interest, Fig. 2 shows Raman spectra of 150 $g{\cdot}kg^{-1}$ aqueous solution of glucose, 150 $g{\cdot}kg^{-1}$ aqueous solution of xylose and an aqueous mixture of 150 $g{\cdot}kg^{-1}$ of each sugar in the spectral region 100–1600 cm^{-1}. These spectra provide evidence regarding the presence of distinguishable peaks for each constituent, allowing for quantitative analysis and the development of univariate models. Thus, considering the mixture spectra in the low wavenumber region, a band at 535 cm^{-1} is observed for xylose which corresponds to C–C–C bending and ring deformation. The band at 445 cm^{-1} arises from the same latter reasons for glucose, the bending of C–C-O at the $–CH_2OH$ group gives the peak at 350 cm^{-1}. At the anomeric region (where the anomeric carbon is involved), the bending of O-C-O for xylose is identified at 600 cm^{-1} and the stretching of C-O at 845 cm^{-1} for glucose. In the fingerprint region, the peak at 980 cm^{-1} for xylose arises from bending of C-O–H bonds [31].

3.2. Univariate and multivariate calibration modeling

Although specific peaks can be isolated as described in the previous section, the most intense regions in the mixture spectrum cannot be exploited due to the hindrance of sugars between each other. An example of the correlation between the raw intensity of the band at 445 cm^{-1} attributed to glucose and the reference concentration of glucose for the first system (glucose and xylose in water) is showed in SM (**Figure S.2**). This result demonstrates the linear correlation between the intensity and the concentration but points out, the importance of spectral pretreatments for univariate modeling.

Fig. 3 presents the selected peaks for univariate models' development after pretreatments. For the quantification of glucose, the spectrum of 100 $g{\cdot}kg^{-1}$ xylose is subtracted from the spectra prior to derivation to avoid the peaks overlaps since both sugars (xylose and glucose) have very close chemical structures. The feed composition used for the breakthrough curves tests was limited to 100 g $kg^{-1}$of each sugar as well.This reduces xylose contributions in the mixture spectra and makes glucose unique peaks more apparent and therefore improve univariate modeling as displayed in Fig. 3: **A** for the first system and **C** for the second system. The spectral range 1115–1215 cm^{-1} is used to quantify glucose at 1140 cm^{-1}. Identical methodology is used to build the rest of univariate models to identify a unique peak for each constituent. The peak around 990 cm^{-1} is chosen when xylose is dissolved in water (Fig. 3B) and for the second system, when ethanol is added to the mixture leading to increased overlapping, the band around 610 cm^{-1} is used instead (Fig. 3D and Fig. 4). Finally, ethanol concentration is monitored by using the intense 888 cm^{-1} peak resulting from stretching of C–C bond, with the subtraction of the xylose spectrum as shown in Fig. 3E.

To go further, multivariate modeling using PLS regression was applied to predict the molecules of interest, and to compare the performance with univariate models. The results of the PLS models developed to predict glucose and xylose with and without ethanol in the mixture are presented in Table 1. The regression plots are shown in Fig. 5. It can be observed that the five models have high R^2 value, over 0.997, and acceptable gaps between RMSEC and RMSECV are obtained for both sugars reflecting good quality. Differences of 0.1 $g{\cdot}kg^{-1}$ and 0.5 $g{\cdot}kg^{-1}$ are calculated for glucose and xylose respectively in absence of ethanol in the solution and 3 LV are used. In case of the second system, gaps of 1.2 $g{\cdot}kg^{-1}$ and 0.8 $g{\cdot}kg^{-1}$ are found, and 5 LV are employed to create the monosaccharides' models. The best ethanol model is built with 8 LV and a difference of 2.4 $g{\cdot}kg^{-1}$ between RMSEC and RMSECV (2.4 $g{\cdot}kg^{-1}$) is obtained.

Overall, PLS modeling lowers RMSEC values and improve correlation coefficients compared to univariate models which suggest better predictions. The comparison of calibration results obtained with univariate and multivariate modeling with the reference concentrations is presented in Fig. 5. Both methods yield similar results with slight improvements using PLS modeling. This improvement can be seen for instance in the calibration data of the system with ethanol which contains mixtures with fixed concentrations of 100 $g{\cdot}kg^{-1}$ glucose and 100 $g{\cdot}kg^{-1}$ xylose with ethanol content ranging from 10 % to 60 %. Fig. 5C shows that univariate model at 100 $g{\cdot}kg^{-1}$ glucose predicts concentrations ranging from 92 $g{\cdot}kg^{-1}$ to 109 $g{\cdot}kg^{-1}$. The addition of ethanol dampens glucose signature peaks which results in the decrease of the measured concentration. PLS model gives more accurate measurements

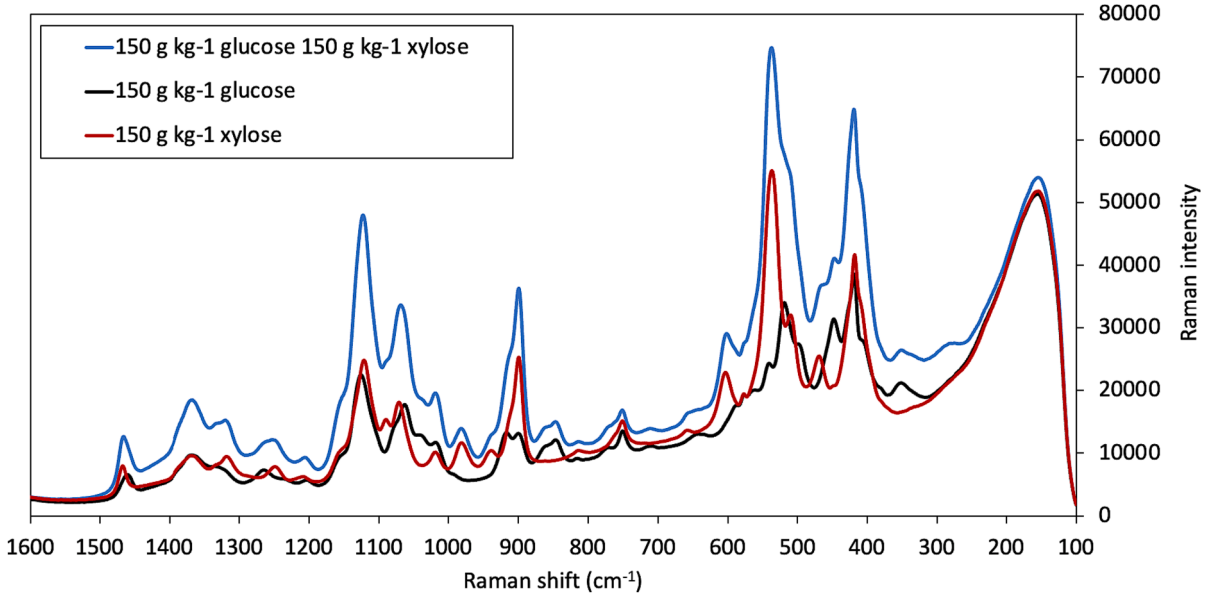

Fig. 2. Raw Raman spectra of individual aqueous sugar solutions and a mixture of glucose and xylose in the spectral region 1600–100 cm^{-1}.

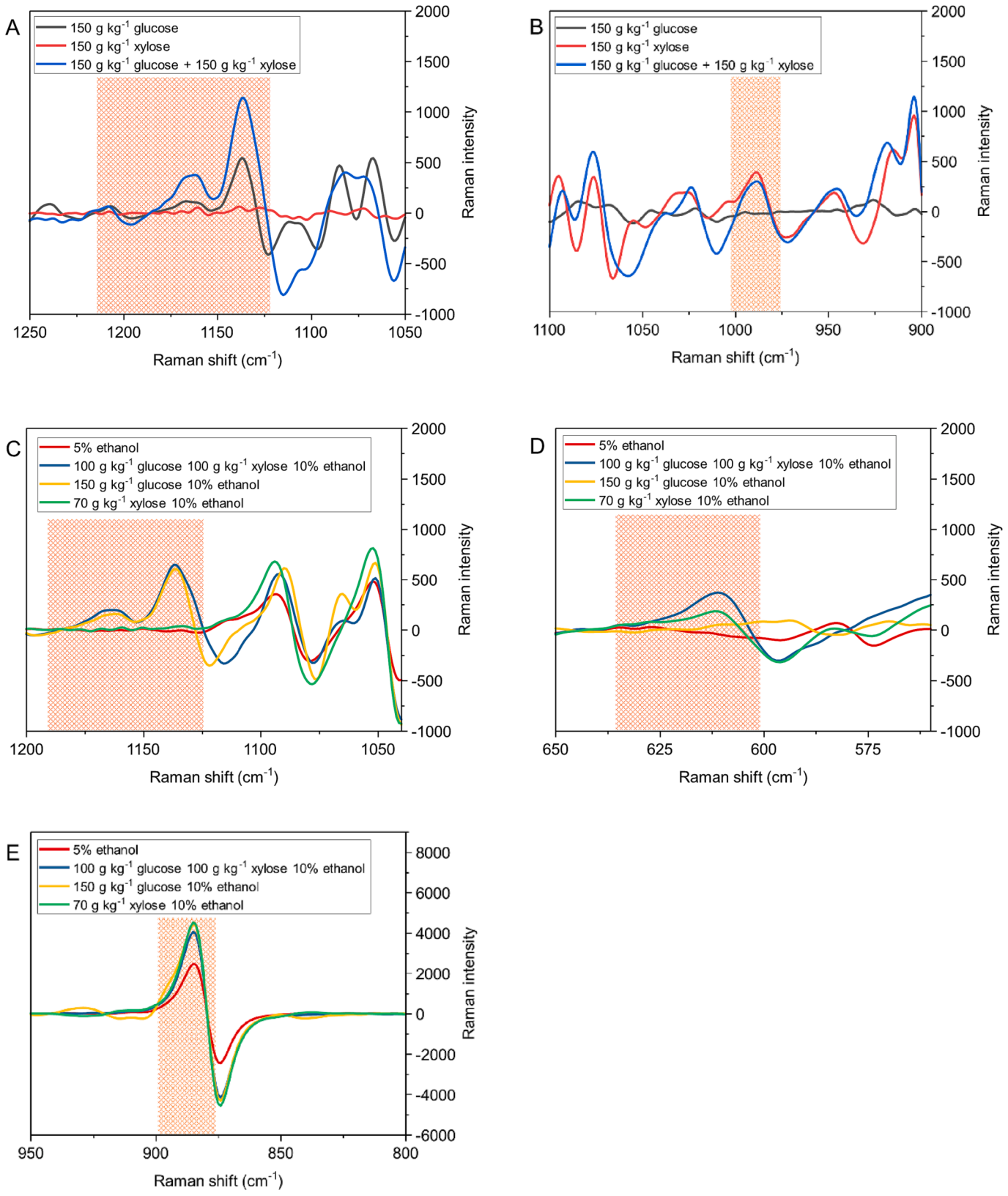

Fig. 3. Pretreated Raman spectra to identify characteristic peaks for (A) glucose, (B) xylose dissolved in water and (C) glucose, (D) xylose, (E) ethanol in the ternary system.

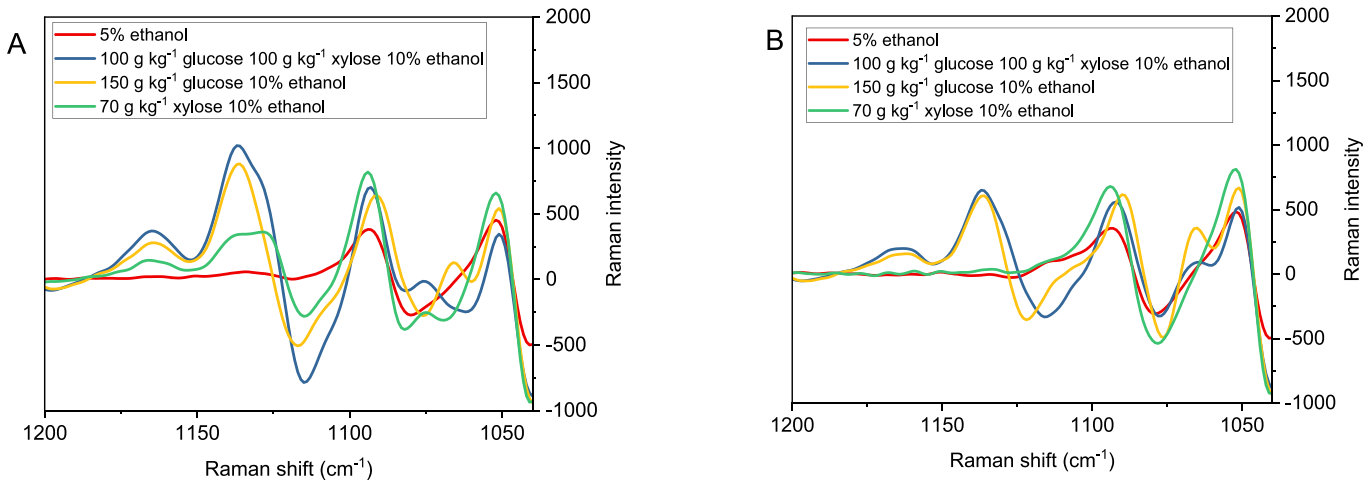

Fig. 4. Spectral subtraction effect on univariate modeling to isolate glucose peak (1115–1215 cm^{-1}) in presence of ethanol. (A) spectra with first derivative and without subtraction of the spectrum of 100 g·kg^{-1} xylose aqueous solution, the model has a correlation coefficient (R2) of 0.976 and a calibration error RMSEC of 47.1866 g·kg^{-1} (B) spectra with first derivative and subtraction of the spectrum of 100 g·kg^{-1} xylose aqueous solution, the model has a correlation coefficient (R2) of 0.989 and a calibration error RMSEC of 2.4774 g·$kg^{-1.}$

Table 1
Univariate and multivariate calibration results.

		Univariate		PLS			
	Concentration range (g·kg^{-1})	RMSEC	R^2	LV	RMSEC	RMSECV	R^2 cal.
glucose / xylose							
glucose	15 – 150	2.7000	0.996	3	2.5614	2.6622	0.997
xylose	15 – 250	3.4764	0.997	3	2.8912	3.4278	0.998
glucose / xylose / ethanol							
glucose	5 – 150	2.4774	0.989	5	1.2330	2.4384	0.999
xylose	5 – 100	2.2750	0.994	5	1.4068	2.2392	0.999
ethanol	10 – 480	3.7435	0.996	8	1.3200	3.6855	0.999

since it is built from information in the selected spectral range rather than from one peak compared to univariate modeling. This information is related not only to glucose but also to variations of the other components in the spectra. A curvature at high ethanol concentrations can be seen for the univariate model (Fig. 5E). This indicates that at high ethanol concentrations, the chosen peak saturates the detector, giving PLS modeling a useful application in this case because it explores additional regions. However, for the low concentration range (0—–300 g·kg^{-1}) the univariate model stays linear with no saturation impact which results in choosing this model for further validation.

3.3. Models validation

To validate the approach, the application of the developed models on an external dataset, meaning that it has not been used to calibrate the models, is mandatory. In this work, we used representative datasets by recording Raman spectra during actual breakthrough experiments using the two systems mentioned above as feed solutions. Working with the acquisition parameters detailed in the experimental section resulted into 108 points per breakthrough curve in 55 min. In parallel, around 50 samples were collected during each experiment and analyzed with HPLC. Since the sampling time of HPLC and the acquisition times of recorded Raman data do not match, we could not calculate the Root Mean Square Errors of Prediction (RMSEP) values taking the HPLC results as references as it is normally done. Thus, to validate and evaluate the predictive quality of the models, the first statistical moment (Equation (1) was calculated and compared for both analytical methods. Two breakthrough experiments were performed, the first was a test with an aqueous mixture of 100 g·kg^{-1} glucose and 100 g·kg^{-1} xylose, the second with 100 g·kg^{-1} glucose, 100 g·kg^{-1} xylose and 50 g·kg^{-1} ethanol.

Fig. 6 shows the precited breakthrough curves employing the developed univariate and PLS models. The latter give smoother curves compared to univariate predictions for sugars. Nonetheless, the opposite observation is found for ethanol. In the case of the first system, univariate models presented in Fig. 6A predict xylose and glucose first moments of 19.8 min and 22.5 min respectively. These results match well with the μ values determined with HPLC (19.8 min and 22.4 min for xylose and glucose respectively). A good agreement is found as well with univariate models in presence of ethanol. Fig. 6C shows first moments of 18.2, 20.4 and 23.5 min for ethanol, xylose, and glucose respectively versus 18.1, 20.3 and 23.3 min with HPLC in the same latter order.

First moments of 19.9 min and 22.3 min are obtained for xylose and glucose respectively in case of the first system as shown in Fig. 6B using PLS models. When ethanol is added to the mixture (Fig. 6D), values of 18.1, 20.4 and 23.3 min are found for ethanol, xylose, and glucose respectively. Overall, chemometric models give close results relative to HPLC and no major improvements are observed compared to univariate models. Less than 1 % error is obtained for all models compared to HPLC curves. The beginnings of the curves at the start of the breakthrough, when solutes start to exit the column, are well predicted, Raman spectroscopy is known to be limited at low concentrations because of low signal to noise ratios and signal decrease with water and ethanol [32]. Nevertheless, PLS model for ethanol does not fit perfectly at the beginning and the end of the curve, ie. when adsorption equilibrium is reached, this is most likely due to a mismodeling of the calibration set. The concentration range of ethanol calibration set is large (ranging from 10 g·kg^{-1} to 480 g·kg^{-1}), which can negatively impact the models' development. Therefore, it is recommended as shown in some studies in the literature to use separate calibrations sets for high and low

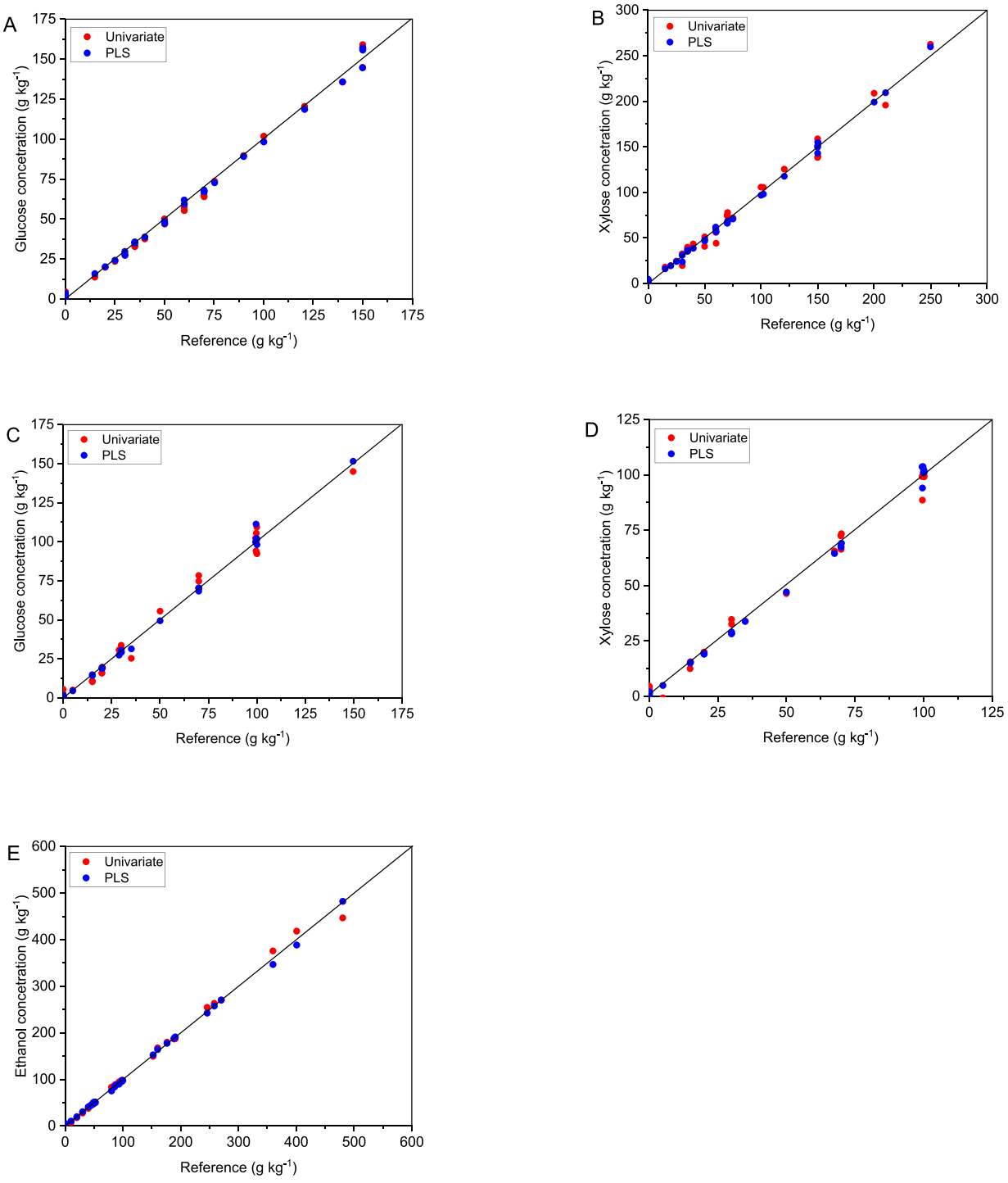

Fig. 5. Regression plots for univariate and multivariate models for (A) glucose, (B) xylose dissolved in water and, (C) glucose, (D) xylose and (E) ethanol in the ternary system.

concentrations in order to improve the accuracy [33–35].

In the two breakthrough experiments, xylose curve precedes glucose one indicating that the adsorbent has an affinity to glucose which delays its exit from the column. In Fig. 6A and Fig. 6B, the two components breakthrough the column at the same time around 12 min and the adsorption equilibrium is established at 34 min for xylose and 40 min for glucose. In case of the second system, ethanol exits the column at 7 min, xylose, and glucose at 11 min. The adsorption equilibrium is established at 25, 34 and 43 min for ethanol, xylose, and glucose respectively. The addition of 5 % ethanol increases the first moment of both sugars from 19.8 min to 20.3 min for xylose and from 22.4 min to 23.3 min for glucose. Consequently, the adsorbed amounts will also increase. This cosolvent effect was shown in the literature when studying the adsorption of sucrose in faujasite-type zeolites, the authors used the batch method for the adsorption study [36].

4. Conclusions

This work demonstrates the employment of Raman spectroscopy for online monitoring of adsorption breakthrough experiments for sugars

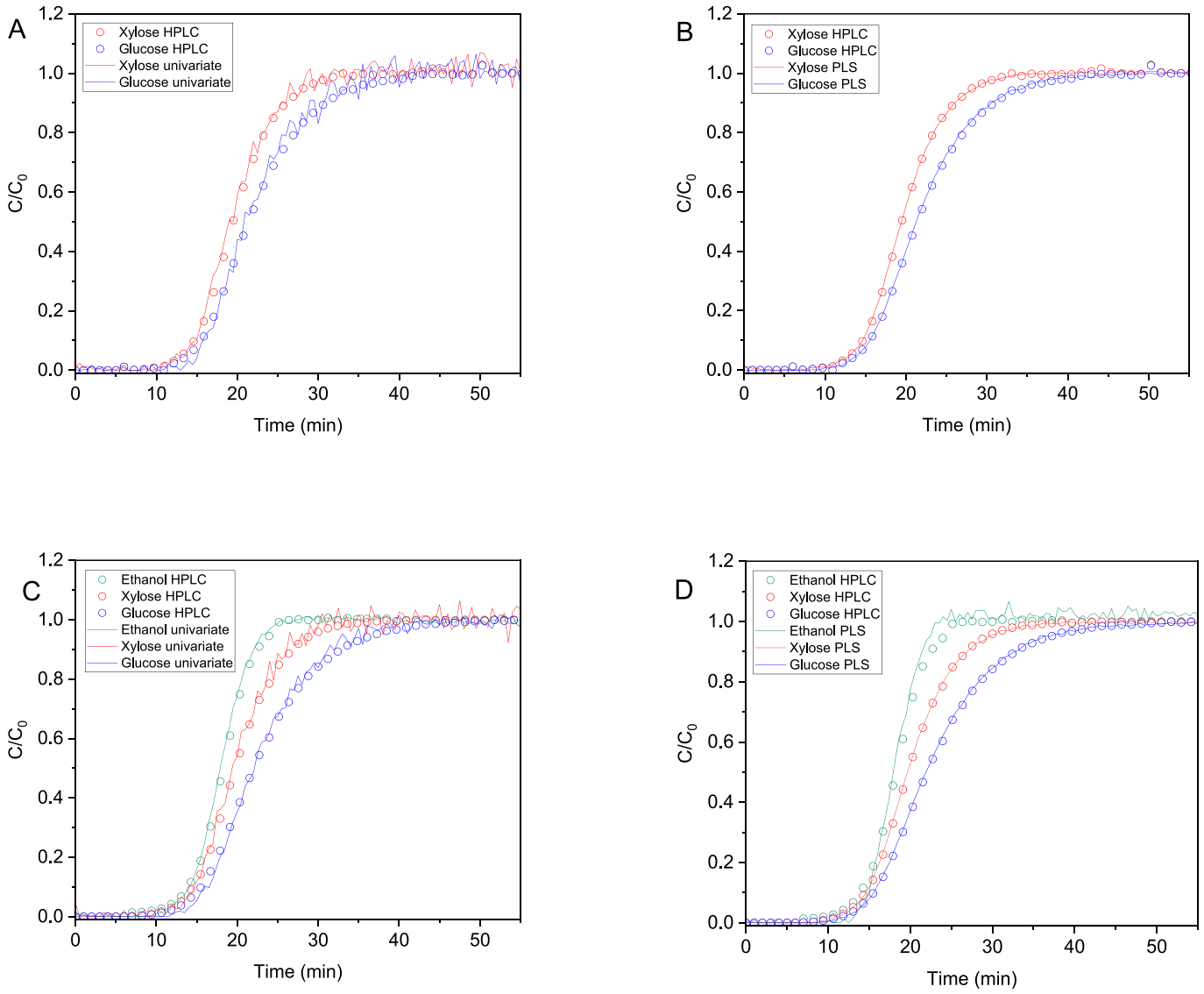

Fig. 6. Breakthrough curves predictions with univariate and PLS models compared to HPLC curves.

separation. Adsorption of lignocellulosic monosaccharides, glucose, and xylose in a BaY zeolite with and without ethanol in the feed mixture was studied. Univariate and multivariate models proved accurate compared to reference HPLC analysis. Univariate models, which are simple to implement, provide robust results at the concentration range used in this study (from 0 to 100 $g{\cdot}kg^{-1}$ for sugars). Preprocessing is essential to enhance accuracy and to avoid overlapping interference in the measurements, first derivative coupled with spectral subtraction of non-targeted components proved to be efficient to develop univariate models. The developed methods can be applied to screen different adsorbents in order to evaluate their potential for a separation application. The presented approaches can be extended to monitor more complex matrixes containing more than two sugars.

CRediT authorship contribution statement

Wassim Ammar: . **Marion Lacoue-Negre:** Writing – review & editing, Writing – original draft, Supervision, Conceptualization. **Alain Methivier:** Supervision, Project administration, Conceptualization. **Maria Manko:** Writing – review & editing, Writing – original draft, Supervision, Conceptualization.

Declaration of competing interest

The authors declare that they have no known competing financial interests or personal relationships that could have appeared to influence the work reported in this paper.

Data availability

The authors do not have permission to share data.

Acknowledgements

The authors would like to thank Arkema for providing the shaped zeolite.

Appendix A. Supplementary data

Supplementary data to this article can be found online at https://doi.org/10.1016/j.saa.2024.123868.

References

[1] O. Rosales-Calderon, V. Arantes, A review on commercial-scale high-value products that can be produced alongside cellulosic ethanol, Biotechnol. Biofuels 12 (2019) 240.

[2] M. Bilal, M. Asgher, H.M.N. Iqbal, H. Hu, X. Zhang, Biotransformation of lignocellulosic materials into value-added products-A review, Int. J. Biol. Macromol. 98 (2017) 447–458.

[3] F.H. Isikgor, C.R. Becer, Lignocellulosic biomass: a sustainable platform for the production of bio-based chemicals and polymers, Polym. Chem. 6 (2015) 4497–4559.

[4] X. Tong, Y. Ma, Y. Li, Biomass into chemicals: Conversion of sugars to furan derivatives by catalytic processes, Appl. Catal. A: General 385 (2010) 1–13.

[5] M. Zheng, J. Pang, R. Sun, A. Wang, T. Zhang, Selectivity control for cellulose to diols: dancing on eggs, ACS Catal. 7 (2017) 1939–1954.

[6] P.Y. Pontalier, A. Ismail, M. Ghoul, Mechanisms for the selective rejection of solutes in nanofiltration membranes, Sep. Purif. Technol. 12 (1997) 175–181.

[7] E. Sjöman, M. Mänttäri, M. Nyström, H. Koivikko, H. Heikkilä, Xylose recovery by nanofiltration from different hemicellulose hydrolyzate feeds, J. Membr. Sci. 310 (2008) 268–277.

[8] W.R. Neuzil, J.W. Priegnitz, Process for separating a ketose from an aldose by selective adsorption, United States, Patent 4 (340) (, 1982) 724.

[9] A. Khosravanipour Mostafazadeh, M. Sarshar, S. Javadian, M.R. Zarefard, Z. Amirifard Haghighi, Separation of fructose and glucose from date syrup using resin chromatographic method: Experimental data and mathematical modeling, Sep. Purif. Technol. 79 (2011) 72–78.

[10] J. Vanneste, S. de Ron, S. Vandecruys, S.A. Soare, S. Darvishmanesh, B. van der Bruggen, Techno-economic evaluation of membrane cascades relative to simulated moving bed chromatography for the purification of mono- and oligosaccharides, Sep. Purif. Technol. 80 (2011) 600–609.

[11] R.C. Kuhn, F. Maugeri Filho, Separation of fructooligosaccharides using zeolite fixed bed columns, J. Chromatogr. B 878 (2010) 2023–2028.

[12] J.P. Stanford, P.H. Hall, M.R. Rover, R.G. Smith, R.C. Brown, Separation of sugars and phenolics from the heavy fraction of bio-oil using polymeric resin adsorbents, Sep. Purif. Technol. 194 (2018) 170–180.

[13] J.A. Vente, H. Bosch, A.B. de Haan, P.J.T. Bussmann, Comparison of sorption isotherms of mono- and disaccharides relevant to oligosaccharide separations for Na, K, and Ca loaded cation exchange resins, Chem. Eng. Commun. 192 (2005) 23–33.

[14] R. Nitzsche, A. Gröngröft, M. Kraume, Separation of lignin from beech wood hydrolysate using polymeric resins and zeolites – Determination and application of adsorption isotherms, Sep. Purif. Technol. 209 (2019) 491–502.

[15] M. Heper, L. Türker, N.S. Kincal, Sodium, ammonium, calcium, and magnesium forms of zeolite Y for the adsorption of glucose and fructose from aqueous solutions, J. Colloid Interface Sci. 306 (2007) 11–15.

[16] C. Ho, C.B. Ching, D.M. Ruthven, A comparative study of zeolite and resin adsorbents for the separation of fructose-glucose mixtures, Ind. Eng. Chem. Res. 26 (1987) 1407–1412.

[17] D.M. Ruthven. Principles of adsorption and adsorption procesesses, John Wiley and Sons, 1994.

[18] J. Ramos, T.C. Duarte, A. Rodrigues, I.J. Silva, C.L. Cavalcante, D. Azevedo, On the production of glucose and fructose syrups from cashew apple juice derivatives, J. Food Eng. 102 (2011) 355–360.

[19] D.A. Luz, A.K.O. Rodrigues, F.R.C. Silva, A.E.B. Torres, C.L. Cavalcante, E.S. Brito, D.C.S. Azevedo, Adsorptive separation of fructose and glucose from an agroindustrial waste of cashew industry, Bioresour. Technol. 99 (2008) 2455–2465.

[20] C. Feller, M. Fink, Refraction as a measure of soluble carbohydrates in storage roots of asparagus, HortScience 42 (2007) 57–60.

[21] A.M. Lines, P. Tse, H.M. Felmy, J.M. Wilson, J. Shafer, K.M. Denslow, A.N. Still, C. King, S.A. Bryan, Online, real-time analysis of highly complex processing streams: quantification of analytes in hanford tank sample, Ind. Eng. Chem. Res. 58 (2019) 21194–21200.

[22] J.S. Lupoi, S. Singh, B.A. Simmons, R.J. Henry, Assessment of lignocellulosic biomass using analytical spectroscopy: an evolution to high-throughput techniques, Bioenergy Res. 7 (2014) 1–23.

[23] J.S. Lupoi, E. Gjersing, M.F. Davis, Evaluating lignocellulosic biomass, its derivatives, and downstream products with Raman spectroscopy, Front. Bioeng. Biotechnol. 3 (2015) 50.

[24] H.E. Lackey, H.A. Colburn, M.V. Olarte, T. Lemmon, H.M. Felmy, S.A. Bryan, A. M. Lines, On-line raman measurement of the radiation-enhanced reaction of cellobiose with hydrogen peroxide, ACS Omega 6 (2021) 35457–35466.

[25] C.-J. Shih, J.S. Lupoi, E.A. Smith, Raman spectroscopy measurements of glucose and xylose in hydrolysate: role of corn stover pretreatment and enzyme composition, Bioresour. Technol. 102 (2011) 5169–5176.

[26] R. Schalk, A. Heintz, F. Braun, G. Iacono, M. Rädle, N. Gretz, F.-J. Methner, T. Beuermann, Comparison of raman and mid-infrared spectroscopy for real-time monitoring of yeast fermentations: a proof-of-concept for multi-channel photometric sensors, Appl. Sci. 9 (2019) 2472.

[27] R. Schalk, F. Braun, R. Frank, M. Rädle, N. Gretz, F.-J. Methner, T. Beuermann, Non-contact Raman spectroscopy for in-line monitoring of glucose and ethanol during yeast fermentations, Bioprocess Biosyst. Eng. 40 (2017) 1519–1527.

[28] C.-J. Shih, E.A. Smith, Determination of glucose and ethanol after enzymatic hydrolysis and fermentation of biomass using Raman spectroscopy, Anal. Chim. Acta 653 (2009) 200–206.

[29] S.R. Gray, S.W. Peretti, H.H. Lamb, Real-time monitoring of high-gravity corn mash fermentation using in situ raman spectroscopy, Biotechnol. Bioeng. 110 (2013) 1654–1662.

[30] S. Wold, M. Sjostrom, L. Eriksson, PLS-regression: a basic tool of chemometrics, Chemom. Intel. Lab. Syst. 58 (2001) 109–130.

[31] M. Dudek, G. Zajac, E. Szafraniec, E. Wiercigroch, S. Tott, K. Malek, A. Kaczor, M. Baranska, Raman optical activity and raman spectroscopy of carbohydrates in solution, Spectrochim. Acta A Mol. Biomol. Spectrosc. 206 (2019) 597–612.

[32] S. Sivakesava, J. Irudayaraj, A. Demirci, Monitoring a bioprocess for ethanol production using FT-MIR and FT-Raman spectroscopy, J. Ind. Microbiol. Biotechnol. 26 (2001) 185–190.

[33] L. Shao, B. Liu, P.R. Griffiths, A.B. Leytem, Using multiple calibration sets to improve the quantitative accuracy of partial least squares (PLS) regression on open-path Fourier transform infrared (OP/FT-IR) spectra of ammonia over wide concentration ranges, Appl. Spectrosc. 65 (2011) 820–824.

[34] S. Alison Arnold, L. Matheson, L.H. Harvey, B. McNeil, Temporally segmented modelling: a route to improved bioprocess monitoring using near infrared spectroscopy? Biotechnol. Lett. 23 (2001) 143–147.

[35] M. Alcalà, J. León, J. Ropero, M. Blanco, R.J. Romañach, Analysis of low content drug tablets by transmission near infrared spectroscopy: selection of calibration ranges according to multivariate detection and quantitation limits of PLS models, J. Pharm. Sci. 97 (2008) 5318–5327.

[36] I. Fornefett, D. Rabet, C. Buttersack, K. Buchholz, Adsorption of sucrose on zeolites, Green Chem. 18 (2016) 3378–3388.